Molecular Pharmacology Fast Forward. Published on May 28, 2013 as doi: 10.1124/mol.113.085696
This article has not been copyedited and formatted. The final version may differ from this version.

MOL #85696

The Neuroactive Steroid Pregnenolone Sulfate Stimulates Trafficking of Functional NMDA Receptors to the Cell Surface via a Non-Canonical G-Protein and Ca^{++} Dependent Mechanism

EMMANUEL KOSTAKIS, CONOR SMITH, MING-KUEI JANG, STELLA C. MARTIN, KYLE G. RICHARDS, SHELLEY J. RUSSEK, TERRELL T. GIBBS and DAVID H. FARB

Laboratory of Molecular Neurobiology, Department of Pharmacology & Experimental Therapeutics, Boston University School of Medicine, 72 East Concord Street, Boston, Massachusetts 02118, USA

Molecular Pharmacology Fast Forward. Published on May 28, 2013 as DOI: 10.1124/mol.113.085696
This article has not been copyedited and formatted. The final version may differ from this version.

Running title: Pregnenolone sulfate increases active surface NMDARs

Corresponding authors:

David H. Farb, Department of Pharmacology, Boston University School of Medicine, 72 East Concord Street, Boston MA 02118, dfarb@bu.edu

Abstract: 249 words

Introduction: 545 words

Discussion: 1609 words

References: 65

Figures: 10

Pages: 46

Abbreviations: (1*S*,3*R*)-1-amino-cyclopentane-1,3-dicarboxylic acid, ACPD; 9-aminoacridine; 9-AA; botulinum toxin type A, BoNT; brefeldin A, BFA; long-term potentiation, LTP; NMDA, N-methyl D-aspartate; NMDAR, NMDA receptor; PKC, protein kinase C; PLC, phospholipase C; PMA, phorbol 12-myristate 13-acetate; PregS, pregnenolone sulfate; PTx, pertussis toxin; HRP, horse radish peroxidase; SMD1, steroid modulatory domain 1; VCP, valosin containing protein

Abstract

NMDA receptors (NMDARs) mediate fast excitatory synaptic transmission and play a critical role in synaptic plasticity associated with learning and memory. NMDAR hypoactivity has been implicated in the pathophysiology of schizophrenia, and clinical studies reveal reduced negative symptoms of schizophrenia with a dose of pregnenolone that elevates serum levels of the neuroactive steroid pregnenolone sulfate (PregS). This report describes a novel process of delayed onset potentiation whereby PregS approximately doubles the cell's response to NMDA via a mechanism that is pharmacologically and kinetically distinct from rapid positive allosteric modulation by PregS. The number of functional cell surface NMDARs in cortical neurons increases 60 -100% within 10 min of exposure to PregS as shown by surface biotinylation and affinity purification. Delayed onset potentiation is reversible and selective for expressed receptors containing the NR2A or NR2B, but not NR2C or NR2D, subunits. Moreover, substitution of NR2B J-K helices and M4 domain with the corresponding region of NR2D ablates rapid allosteric potentiation of the NMDA response by PregS but not delayed onset potentiation. This demonstrates that the initial phase of rapid positive allosteric modulation is not a first step in NMDAR upregulation. Delayed onset potentiation by PregS occurs via a non-canonical, pertussis toxin sensitive G-protein coupled and Ca^{2+} dependent mechanism that is independent of NMDAR ion channel activation. Further investigation into the sequelae for PregS stimulated trafficking of NMDARs to the neuronal cell surface may uncover a new target for the pharmacological treatment of disorders in which NMDAR hypofunction has been implicated.

Molecular Pharmacology Fast Forward. Published on May 28, 2013 as DOI: 10.1124/mol.113.085696
This article has not been copyedited and formatted. The final version may differ from this version.

Introduction

NMDARs play a critical role in synaptic plasticity underlying learning and memory, in part by dynamically regulating the trafficking of AMPA receptors via NMDAR channel mediated Ca^{2+} transport into dendritic spines. NMDA receptor trafficking is also regulated in response to neuronal activity, via both phosphorylation-dependent and phosphorylation-independent pathways (Chen and Roche, 2007; Lau et al., 2009).

NMDAR antagonists reproduce both the positive and negative symptoms of schizophrenia in humans and worsen the symptoms of nonmedicated patients (Gaspar et al., 2009), suggesting that NMDAR hypofunction contributes to the symptoms of schizophrenia. Consistent with this hypothesis, enhancing NMDAR function by administering agonists acting at the NMDAR glycine site has been reported to be effective in reducing symptoms of schizophrenia (Labrie and Roder, 2009). The negative symptoms of schizophrenia, including cognitive deficits, blunted affect, poverty of speech, anhedonia, asociality, and lack of motivation, are highly predictive of poor clinical outcome (Milev et al., 2005), and are largely refractory to conventional antidopaminergic pharmacotherapy. Pharmacological options for enhancing NMDAR function are currently limited to acute agonism of receptor activity.

The results of clinical trials indicate that the positive and negative symptoms of schizophrenia are ameliorated in patients receiving adjunctive treatment with pregnenolone (Marx et al., 2011), concordant with elevated serum levels of the neuroactive steroid PregS (Marx et al., 2009). PregS enhances learning and memory in animal models (Gibbs et al., 2006; Marx et al., 2011) and enhances LTP at hippocampal CA1 synapses (Chen et al., 2007; Sabeti et al., 2007; Sliwinski et al., 2004). PregS at micromolar concentrations acts as an allosteric modulator for a

Molecular Pharmacology Fast Forward. Published on May 28, 2013 as DOI: 10.1124/mol.113.085696
This article has not been copyedited and formatted. The final version may differ from this version.

variety of neurotransmitter receptors, including glutamate, glycine, and $GABA_A$ receptors (Wu et al., 1991; Majewska and Schwartz, 1987). In particular, PregS enhances activation of NMDARs containing NR2A (NR1/2A receptors) or NR2B (NR1/2B receptors), while inhibiting receptors containing NR2C (NR1/2C receptors) or NR2D (NR1/2D receptors) (Wu et al., 1991). Rapid enhancement of NMDAR function by PregS is evident on a time scale of seconds, consistent with direct allosteric modulation of cell surface NMDARs (Park-Chung et al., 1997; Wu et al., 1991). Analysis of recombinant NMDAR chimeras expressed in *Xenopus laevis* oocytes (henceforth, oocytes) has identified a steroid modulatory domain and possible PregS binding site on the NR2 subunit that includes the J/K helices in the S2 region of the glutamate recognition site and the contiguous fourth membrane domain (Jang et al., 2004). While exploring the effects of PregS in vivo, we found a higher potency process whereby low nM sulfated steroid released DA from striatal synaptosomes (Whittaker et al., 2008) *ex vivo* and the striatum *in vivo* contingent upon NMDAR activity (Sadri-Vakili et al., 2008). However, the cellular mechanism by which PregS may act at high potency is unknown.

This report shows that PregS pharmacologically stimulates NMDA efficacy by enhancing receptor trafficking to the cell surface. This occurs via a novel target and pathway that is dependent upon intracellular Ca^{2+} signaling but not NMDAR channel activation or entry of extracellular Ca^{2+}. Instead, PregS stimulates release of intracellular Ca^{2+} via a pertussis toxin (PTx) sensitive and phospholipase C (PLC) dependent pathway. Therefore, in addition to ionotropic signaling, NMDARs are capable of regulating their own surface expression through a non-canonical mode of signaling (Rozas et al., 2003) that utilizes an intracellular transduction pathway more typical of GPCRs.

Molecular Pharmacology Fast Forward. Published on May 28, 2013 as DOI: 10.1124/mol.113.085696
This article has not been copyedited and formatted. The final version may differ from this version.

Materials and Methods

Materials. Rat NR1-1a (hereafter referred to as NR1) cDNAs were provided by Dr. S. Nakanishi and the cDNAs of NR2A, NR2B, NR2C, and NR2D subunits were gifts from Dr. P.H. Seeburg. Stock solutions of steroids were prepared in dimethyl sulfoxide (DMSO). Final concentration of DMSO in all buffer and drug solutions was 0.5%. Chemicals were from Sigma Chemical (St. Louis, Missouri). Restriction enzymes were from New England Biolabs (Beverly, Massachusetts).

Preparation of cRNA. Plasmids were linearized with appropriate restriction enzymes prior to *in vitro* transcription using mMESSAGE mMACHINE™ High Yield Capped RNA Transcription kits (Ambion, Inc., Austin, TX). Plasmids containing NMDAR subunits were linearized with NotI (NR1), KpnI (NR2B), or XhoI (NR2A). Linearized DNAs were subjected to phenol/$CHCl_3$ extraction and ethanol precipitation. The T7 in-vitro transcription kit was used for NR1 and NR2A cRNAs and the SP6 kit was used for NR2B cRNAs.

Receptor expression in oocytes. Expression of NMDA and $GABA_A$ receptors in oocytes was carried out as previously described (Kostakis et al., 2011; Berezhnoy et al., 2008). Briefly, oocytes from *Xenopus laevis* frogs (Nasco, Fort Atkinson, Wisconsin) were micro-injected with cRNAs transcribed *in-vitro* from plasmids containing cDNAs of desired NMDAR or $GABA_A$ receptor subunits, and maintained in Barth's solution (in mM): (84 NaCl, 2.4 $NaHCO_3$, 0.82 $MgSO_4$, 1 KCl, 0.33 $Ca(NO_3)_2$, 0.41 $CaCl_2$, 7.5 Tris/HCl, 2.5 pyruvate, 100 U/ml penicillin/streptomycin, pH 7.4) at 18°C for 2 - 4 days before recording.

Oocyte electrophysiology. Two-electrode voltage clamp recordings from oocytes were conducted

Molecular Pharmacology Fast Forward. Published on May 28, 2013 as DOI: 10.1124/mol.113.085696
This article has not been copyedited and formatted. The final version may differ from this version.

(23 - 25°C; holding potential -70 mV) and membrane currents filtered (1 kHz) and digitized and sampled (100 Hz) as described previously (Malayev et al., 2002). $Ca^{2+}$and Mg^{2+} free Ba-Ringer perfusion buffer (mM): 96 NaCl, 2 KCl, 1.8 $BaCl_2$, 5 HEPES, 0.5% DMSO, pH 7.5. NMDA was applied in combination with a saturating concentration of glycine (50 μM). Oocytes were preincubated with externally applied inhibitors in Barth's solution followed by inclusion of inhibitor in the recording solution. PregS was applied as 100 μM, except where indicated, and all concentrations of PregS appeared soluble in 0.5% DMSO.

Data analysis. To pool results from multiple oocytes, baseline responses to NMDA were established and peak NMDA responses in the presence of PregS were expressed to reveal response augmentation. Rapid enhancement of the NMDA response by PregS was defined as $\%P(rapid) = (I_{NMDA+PregS(simultaneous)}/I_{NMDA} - 1) \times 100$, the % increase in peak current (%P) induced by NMDA + PregS, as compared to the peak current induced by application of NMDA in the absence of PregS. For purpose of analysis, delayed enhancement of the NMDA response is defined as $\%P(delayed) = (I_{NMDA+PregS(10\ min)}/I_{NMDA+PregS(simultaneous)} - 1) \times 100$, the percentage increase in the response to NMDA + PregS when applied after a 10 min preincubation with PregS, as compared to the response elicited when NMDA and PregS are applied simultaneously. For example, if rapid potentiation increases the response by 100% and delayed enhancement of the NMDA response also increases the response by an additional 100%, then the NMDA response after a 10 min exposure to PregS is 400% of the response in the absence of PregS. Significance testing was by 2-tailed t-test. EC_{50}s were estimated by nonlinear regression using the logistic equation.

Cell Culture. Primary rat neocortical cultures were prepared from E18 embryos maintained 7

Molecular Pharmacology Fast Forward. Published on May 28, 2013 as DOI: 10.1124/mol.113.085696
This article has not been copyedited and formatted. The final version may differ from this version.

days *in vitro* as described previously (McLean et al., 2000).

Confocal Ca^{2+} imaging of Xenopus oocytes and neocortical cells in culture. Oocytes were injected with 50 nl 1 mM fluo-3 (penta ammonium salt, F1240; Molecular Probes, OR) (Jaconi et al., 1997). Confocal images were acquired in real time using a Zeiss Axiovert 150M laser scanning confocal microscope with a Plan-neofluor 10x/0.3 objective lens at 8 sec per frame. Oocytes were positioned in a 14 mm glass microwell containing 2 ml Ca^{2+}-free Ba-Ringer and the focus was adjusted to image the cross-section of greatest diameter, approximately through the center of the oocyte. Oocytes exhibited a low level of fluorescence in the absence of fluo-3 injection. Gain was adjusted such that fluo-3 injected oocytes exhibited minimal visible fluorescence, and this gain setting was used for all imaging. The oocyte was initially imaged in saline to establish a stable baseline and then 2 ml of PregS in Ba-Ringer was superfused to yield a final concentration of 100 μM PregS. Fluorescence was measured with an argon laser (488 nm wavelength) and an emission filter (band path 505 – 530 nm). The fluorescence signal intensity for each oocyte was calculated using the measurement histogram function of the Carl Zeiss LSM Image Examiner software. Values for each oocyte were divided by the first value from the imaging of that oocyte to give a change in fluorescence from the base line.

Neocortical cells were plated on polylysine treated glass bottom dishes and maintained *in vitro* for 7 days prior to imaging. The cells were incubated for 20 min with Fluo-4 acetoxymethyl ester (AM), the cell permeable ester of the fluorescent calcium indicator (F-14201, Molecular Probes, OR). The confocal images were acquired in real time using a Zeiss Axiovert 150M laser scanning confocal microscope with a C-Apochromat 40x/1.2 40x water immersion objective at 1frame/s. Culture dishes initially contained 2 ml of Ca^{2+}-free HEPES buffered saline. The gain

Molecular Pharmacology Fast Forward. Published on May 28, 2013 as DOI: 10.1124/mol.113.085696
This article has not been copyedited and formatted. The final version may differ from this version.

was kept constant. After baseline imaging, 2 ml of PregS was perfused into the culture dish to yield a final concentration 50 μM. Fluo-4 fluorescence was measured with an argon laser and an emission filter and changes in Ca^{2+} levels were determined as described above.

Labeling and purification of surface proteins. Primary rat neocortical cells were treated for 10 min at room temperature with 100 μM PregS or vehicle (0.1% DMSO) in Ca^{+2}-free HEPES-buffered saline. Cell-surface proteins were biotinylated with membrane-impermeant biotinamidocaproate N-hydroxysuccinamide ester and extracts prepared as described previously (Martin et al., 1999) with the following modifications: cortical cultures were biotinylated for 10 min at 25˚C. Protein extracts were prepared in ice-cold 1% (v/v) Nonidet P-40, 0.1% (w/v) SDS, 10% (v/v) glycerol, 50 mM Tris–HCl, 150 mM sodium chloride with protease inhibitors (Roche). Extract protein concentration was determined and equal amounts of protein from vehicle and PregS-treated cells were retained (Total) for western blotting. Equal amounts of protein from the remaining lysate of each treatment group were affinity-purified with NeutrAvidin Agarose Resin (Thermo Fisher Scientific) at 4˚C overnight, then pelleted and resuspended in extraction buffer three times to remove unbound protein. The final pellet was heated at 80˚C in 1:20 (v/v) β-mercaptoethanol-supplemented Tris-Glycine SDS Sample buffer (Invitrogen) to dissociate the neutravidin-biotin conjugate, and equal volumes of the resulting samples (Biotinylated) were used in western blots.

Antibodies. The following antibodies were used: mouse anti-glutamate receptor NR1 (1:1000 [clone 54.1] BD Pharmingen), mouse anti-sodium potassium ATPase (1:1000 [clone 464.6] Abcam), mouse anti-valosin containing peptide (1:5000 [clone 5] Abcam). Antibodies were detected with the appropriate HRP-conjugated secondary antibody, Protein A-HRP (1: 4000,

Molecular Pharmacology Fast Forward. Published on May 28, 2013 as DOI: 10.1124/mol.113.085696
This article has not been copyedited and formatted. The final version may differ from this version.

Zymed) or goat anti mouse IgG F(ab)2 fragment-HRP (1:4000, Abcam).

Western blots. Protein extracts were separated by SDS polyacrylamide gel electrophoresis on 6% tris-glycine gels, transferred to nitrocellulose membranes (Invitrogen) and polypeptides were detected by immunoblotting followed by enhanced chemiluminescence (GE Healthcare) according to standard methods (Martin et al., 1999). X-ray film (CL-Xposure, Fisher Scientific) was scanned using a Molecular Dynamics Personal Densitometer SI Model 375 and quantified using Image Quant TL software (Amersham Biosciences). Increasing amounts of total protein were run on each gel, probed with anti-NR1 antibody, and quantified to verify that densitometric analysis was performed within the linear range of the detection system. Surface NR1 band intensity was quantified only if band intensity was within the linear range of total NR1 band intensity. Surface protein is defined as the ratio of biotinylated to total protein band intensity, and surface and total protein is expressed as % vehicle-treated control.

Electrophysiological recordings of primary neurons. Dissociated 7-day chick embryo spinal cord neurons (2-4 weeks in culture) were prepared as described (Farb et al., 1979). Whole-cell currents were recorded by as described (Park-Chung et al., 1997). Patch electrodes (5-10 MΩ) filled with intracellular solution containing (in mM) 153 CsCl, 10 EGTA, and 10 HEPES (pH to 7.2 with CsOH). Bath solution (in mM): 150 NaCl, 4 KCl, 1 $CaCl_2$, and 10 HEPES (pH to 7.2 with NaOH). For some experiments, a Ca^{2+}-free solution was used in which 1 mM $BaCl_2$ was substituted for $CaCl_2$ (Ba-buffer). Drug solutions were applied to single neurons (23 - 25°C; holding potential -70 mV) by pressure ejection (15 psi) from seven-barrel borosilicate glass pipettes positioned approximately 50 µm from the neuronal soma.

Molecular Pharmacology Fast Forward. Published on May 28, 2013 as DOI: 10.1124/mol.113.085696
This article has not been copyedited and formatted. The final version may differ from this version.

Results

Enhancement of the NMDA induced current by PregS exhibits rapid and delayed phases

As previously reported (Wu et al., 1991), simultaneous application of NMDA and PregS results in rapid potentiation of the NMDA response of chick spinal cord neurons in culture, reflecting allosteric modulation of NMDAR activation. The peak current response to a 10 s application of 30 μM NMDA + 100 μM PS was increased by 167 ± 29% (n=3) over the response to 30 μM NMDA alone. However, with continued exposure to PregS, a further, delayed phase of potentiation became apparent (Fig. 1A), with the NMDA response after 180 s increased by 359 ± 58% over the initial response to NMDA alone (i.e., 4.6 times the initial NMDA response). Both rapid and delayed enhancement of the NMDA response by PregS are reversible, with the NMDA-induced current returning to control 4.5 min after washout of PregS. Replacement of Ca^{2+} with Ba^{2+} in the extracellular solution had no significant effect ($p > 0.05$, unpaired t-test) on the delayed potentiation the NMDA response by PregS; the response to a 10 s application of NMDA + PregS was increased by 87 ± 36% compared to NMDA alone, which increased to 261 ± 51% potentiation (n = 4) after 180 s of exposure to PregS (Fig. 1B).

To determine whether the delay in enhancement is imposed by the time required for PregS to reach an intracellular target, 100 μM PregS was added to the intracellular buffer in the whole-cell recording electrode to saturate intracellular sites for at least 60 sec after obtaining the whole-cell configuration and before extracellular application of the same concentration of PregS. The time course of PregS potentiation was, however, unaltered ($p > 0.05$, unpaired t-test) by the inclusion of PregS in the intracellular solution (Fig. 1C). Potentiation by PS was 128 ± 40% after 10 s and 481 ± 140% (n = 4) after 180 s, arguing that delayed potentiation, like rapid

Molecular Pharmacology Fast Forward. Published on May 28, 2013 as DOI: 10.1124/mol.113.085696
This article has not been copyedited and formatted. The final version may differ from this version.

potentiation, is mediated by a site associated with the extracellular membrane surface.

The NR2 subunit controls the delayed phase of potentiation

NMDARs comprised of various subunit combinations were expressed in oocytes to ask whether the NR2 subunit might affect delayed potentiation. Similar to observations in neurons, both rapid and delayed phases of potentiation are observed. PregS rapidly and reversibly potentiates the peak current elicited by NMDA on cells expressing NR1/2A receptors. However, the NMDA response continues to increase with a time constant of ~3 min, resulting in a total potentiation of 200 - 370% (Fig. 2A, B). The delayed onset NMDA response returns to control 2 - 3 min after removal of PregS, showing that delayed potentiation is reversible (Fig. 2B). Whereas the response to application of NMDA alone typically exhibited a rapid rise and a "flat-topped" response profile that was stable over a 10 s application interval, responses in the presence of PregS typically exhibited a profile with a slight upward slope, likely reflecting the progress of delayed potentiation (Fig. 2A). Repetitive application of NMDA as shown in Figs. 1 and 2 was not necessary as application of PregS for 10 min prior to NMDA + PregS was sufficient to elicit delayed potentiation. For subsequent experiments, the magnitudes of rapid and delayed potentiation were assessed by comparing the response to NMDA alone, the response to NMDA + PregS, and the response to NMDA + PregS applied after 10 min of exposure to PregS.

Delayed potentiation of the NMDA response by PregS is observed in oocytes expressing NR1/2A or NR1/2B receptors but not in oocytes expressing NR1/2C or NR1/2D receptors (Fig 3A). This is in contrast to rapid modulation, wherein PregS initiates rapid positive modulation of NR1/2A and NR1/2B receptors but negative modulation of NR1/2C and NR1/2D receptors (Malayev et al., 2002). In the case of NR1/2A receptors, the concentration-response curve for

Molecular Pharmacology Fast Forward. Published on May 28, 2013 as DOI: 10.1124/mol.113.085696
This article has not been copyedited and formatted. The final version may differ from this version.

delayed potentiation by PregS exhibits a 25-fold greater potency (EC_{50} 850 nM) than for rapid potentiation (EC_{50} 21 μM) (Fig. 3B). Thus, PregS exhibits substantial potentiation and selectivity at a much lower concentration: at100 nM PregS (Fig. 3B) there is substantial delayed potentiation yet little or no rapid potentiation. By contrast, in the case of NR1/2B receptors, 100 nM PregS exhibits no detectable delayed or rapid potentiation (Fig. 3C).

Delayed potentiation is independent of rapid potentiation

The observation that the PregS EC_{50} for delayed potentiation of NR1/2A receptors is 25-fold lower than for rapid potentiation suggests that rapid and delayed potentiation are independent processes. As shown in Figure 4, PregS at a concentration of 100 nM produces no rapid potentiation of the 10 μM NMDA response of NR1/2A receptors, yet nevertheless induces 45 ± 3% delayed potentiation.

As previously reported, rapid PregS potentiation is eliminated in NR1-1a/χ4 receptors, where χ4 is a chimeric NR2 subunit in which steroid modulatory domain 1 (SMD1) encompassing the J-K helices and the M4 domain (S759–I836) of NR2B is replaced with the equivalent region of NR2D (Jang et al., 2004). As shown in figure 3A, delayed potentiation by PregS persists with this construct, arguing that delayed potentiation is not contingent on rapid positive allosteric modulation and acts via a novel NMDAR site that is independent of SMD1.

$GABA_A$ receptors do not exhibit delayed potentiation

To determine whether delayed potentiation is limited to NMDARs, α1β2γ2s $GABA_A$ receptors and NR1/2A receptors were co-expressed in oocytes. Whereas the response to 300 μM NMDA was enhanced when NMDA was applied in combination with 100 μM PregS, the response to

Molecular Pharmacology Fast Forward. Published on May 28, 2013 as DOI: 10.1124/mol.113.085696
This article has not been copyedited and formatted. The final version may differ from this version.

GABA was substantially inhibited but still readily measurable. Moreover, whereas a 10 min pre-exposure of oocytes to PregS produced further enhancement of the NMDA response, the amplitude of the GABA response was similar to that observed when GABA and PregS were applied simultaneously, indicating the absence of a delayed effect of PregS on $GABA_A$ receptors (Supplemental Figure 1).

G-protein activation is involved in delayed potentiation

The extended time scale of delayed potentiation suggests the involvement of intracellular signal transduction pathways. To test for GPCR involvement, potentiation by PregS was examined ~4 h after injection of oocytes with 500 pg of pertussis toxin (PTx). Delayed potentiation was significantly diminished in PTx-injected oocytes. To test for the involvement of PLC, we examined the effects of U-73122, an inhibitor of G protein-mediated PLC activation (Smith et al., 1990; Thompson et al., 1991; Smallridge et al., 1992). Oocytes treated with U-73122 (20 μM, 1 h) exhibit reduced responses to NMDA (~10% of control, data not shown), and delayed potentiation is absent. Oocytes treated with the inactive analog U-73343 are unaffected (Table 1). Notably, none of the pharmacological treatments affected rapid potentiation by PregS (Table 1).

PKC mediates delayed but not rapid potentiation

To investigate the role of protein kinases in delayed potentiation by PregS, we examined the effect of PregS in oocytes treated with protein kinase inhibitors and activators. Pretreatment of cells expressing NR1/2A receptors with the PKC activator phorbol 12-myristate 13-acetate (PMA) substantially increases the NMDA response in the absence of PregS (404 ± 19%, n = 8), but does not significantly affect rapid potentiation by PregS, whereas delayed potentiation by

Molecular Pharmacology Fast Forward. Published on May 28, 2013 as DOI: 10.1124/mol.113.085696
This article has not been copyedited and formatted. The final version may differ from this version.

PregS is abolished (Table 2). Because PMA itself enhances the NMDA response (Supplemental Figure 2), this likely reflects saturation of the PKC-dependent pathway by PMA.

Pretreatment of cells with staurosporine, a broad-spectrum inhibitor of serine/threonine protein kinases, does not affect the magnitude of the control NMDA response, but significantly reduces delayed potentiation (Table 2). Similar results are observed with the PKC inhibitor bisindolylmaleimide I. In contrast, the nonreceptor protein kinase inhibitor genistein, the protein kinase inhibitor CK2 (Litchfield, 2003), the casein kinase II inhibitor 5,6-dichloro-1-β-d-ribofuranosylbenzimidazole (DRB), and the MEK inhibitor U0126 are without effect on delayed potentiation. Delayed potentiation by PregS is unaffected by treatment with the insulin receptor tyrosine kinase inhibitor tyrphostin A47 (10 min, 100 μM), which blocks insulin-induced potentiation of the NMDA response (Skeberdis et al., 2001b) (Table 2). None of the inhibitors tested altered rapid potentiation, demonstrating that distinct mechanisms mediate rapid and delayed potentiation.

σ receptors do not mediate delayed potentiation

To test for involvement of σ1 receptors, oocytes were pretreated with the σ receptor ligands BD 1063 (30 μM) or haloperidol (10 μM). Delayed potentiation was unaffected (control: 80 ± 6%, BD-1063, 74 ± 9%, haloperidol: 72 ± 5%; n =6-13), indicating that σ1 receptors do not play a role in potentiation of the NMDA response by PregS.

Delayed potentiation by PregS requires Ca^{2+} release from intracellular stores.

Pharmacological evidence for the involvement of PLC and PKC in delayed potentiation suggests a Ca^{2+} mediated pathway. To evaluate the role of Ca^{2+}, oocytes were injected with EGTA 30 min

Molecular Pharmacology Fast Forward. Published on May 28, 2013 as DOI: 10.1124/mol.113.085696
This article has not been copyedited and formatted. The final version may differ from this version.

prior to recording. As shown in Table 3, delayed potentiation is significantly reduced by intracellular chelation of Ca^{2+}. Because recordings were routinely carried out in Ca^{2+}-free Ba-Ringer, the most likely source of Ca^{2+} is release from intracellular stores. We therefore examined the effect of the endoplasmic reticulum Ca^{2+}-ATPase inhibitor thapsigargin, which depletes Ca^{2+} stores and elevates $[Ca^{2+}]_i$. After incubation with thapsigargin (1 mM for 1 hr), oocytes exhibit ~700% increase in the NMDA current compared to untreated oocytes (data not shown), in agreement with previous reports (Nishizaki et al., 1999; Skeberdis et al., 2001a). Rapid potentiation is unaltered after thapsigargin treatment, but delayed potentiation is eliminated. Delayed potentiation is abolished in oocytes injected with 50 nl of 1mM heparin (Table 3), an inhibitor of the oocyte IP_3 receptor, but persists in control oocytes injected with the inactive analog de-N-sulfated heparin (Noh et al., 1998).

PregS increases intracellular [Ca^{2+}]

To test the hypothesis that PS stimulates release of Ca^{2+} from intracellular stores, $[Ca^{2+}]_i$ was visualized in oocytes by confocal microscopy using fluo-3 (Fig. 5). Oocytes expressing NR1/2A receptors exhibit a transient increase in Ca^{2+} fluorescence beginning within seconds of PregS, but not vehicle, addition, peaking after about 50 sec and subsiding to baseline after 3 - 4 min. PregS had no effect on Ca^{2+} fluorescence in oocytes that were uninjected or injected with vehicle, demonstrating that NMDA receptors are essential for PregS-induced Ca^{2+} release. Oocytes expressing NR1/2D receptors failed to exhibit an increase in Ca^{2+} fluorescence, demonstrating subunit specificity.

The increase in Ca^{2+} fluorescence is primarily localized close to the membrane, consistent with the location of IP_3-releasable Ca^{2+} stores in oocytes (Yao et al., 1995). The PregS-induced

Molecular Pharmacology Fast Forward. Published on May 28, 2013 as DOI: 10.1124/mol.113.085696
This article has not been copyedited and formatted. The final version may differ from this version.

increase in Ca^{2+} fluorescence was observed in Ca^{2+}-free Ba-Ringer, indicating that the increase in $[Ca^{2+}]_i$ fluorescence is due to Ca^{2+} release from intracellular stores, and not entry of Ca^{2+} via NMDAR channels. A control experiment in which an oocyte expressing NR1/2A receptors was exposed to PregS in Ca^{2+}-free/Ba^{2+}-free Ringer containing 1 mM EGTA yielded a similar increase in fluorescence.

To determine whether PregS is similarly capable of increasing intracellular Ca^{2+} in neurons, primary rat neocortical neurons in culture were incubated with the membrane-permeant Ca^{2+} indicator fluo-4 AM and exposed to various concentration of PregS. As shown in Fig. 6, PregS elicits a large initial increase in neuronal Ca^{2+} fluorescence that diminishes with time but persists over baseline for at least three minutes.

Exocytosis is required for delayed potentiation

Delayed potentiation by PregS was blocked by injection of oocytes with botulinum toxin type A (BoNT A), a zinc endoprotease produced by bacteria of the genus *Clostridium* that cleaves SNAP-25 and prevents SNARE regulated exocytosis (Pellizzari et al., 1999; Lan et al., 2001a). Rapid potentiation was insensitive to BoNT A (Fig. 7), indicating that delayed, but not rapid, potentiation requires exocytosis. Treatment with BoNT A alone did not reduce the amplitude of the NMDA response, arguing that most NMDARs do not exhibit rapid recycling in the absence of PregS. Similarly, delayed potentiation was significantly inhibited by Brefeldin A (BFA) (control: 70 ± 3%, BFA: 42 ± 5%, $p < 0.01$, $n = 13$), which disassembles the Golgi complex and inhibits vesicular transport (Oda et al., 1987; Misumi et al., 1986; Klausner et al., 1992).

PregS increases the functional cellular response to NMDA via increasing surface receptors.

Molecular Pharmacology Fast Forward. Published on May 28, 2013 as DOI: 10.1124/mol.113.085696
This article has not been copyedited and formatted. The final version may differ from this version.

To determine whether delayed potentiation is due to an increase in the number of functional NMDARs on the cell membrane, we examined tail currents elicited by a depolarizing voltage jump following complete NMDAR blockade by the open-channel blocker 9-aminoacridine. Block by 9-aminoacridine (9-AA) traps activated NMDARs in a nonconducting state from which the co-agonists NMDA and glycine are unable to dissociate, synchronizing all functional NMDAR channels in a blocked open conformation (Fig. 8A) (Benveniste and Mayer, 1995). Block by 9-AA is voltage dependent, such that a depolarizing voltage step to +70 mV induces rapid (< 3 ms) dissociation of 9-AA, such that all of the NMDAR channels that have accumulated in the blocked state reopen nearly simultaneously after depolarization (Benveniste and Mayer, 1995; Chen et al., 1999). The resulting tail current is independent of the efficacy of NMDA and proportional to the number of activatable receptors (Horak et al., 2006). The amplitude of the tail current after a voltage jump from -70 to +70 mV is more than doubled following 10 min exposure to PregS (Fig. 8B), indicating that the number of functional surface NMDARs is increased. This is similar to the magnitude of delayed potentiation, arguing that delayed potentiation is due to an increase in the number of functional surface receptors.

PregS increases surface NMDARs in neurons.

To determine whether the PregS increases surface NMDARs in neurons, , rat neocortical neurons were exposed to PregS for 10 min and surface proteins labeled with biotin. Following affinity purification on an avidin column, levels of total and biotinylated surface NR1 were assessed by Western blot. As quantified in Fig. 9, PregS increases surface NR1 by 62 ± 25% ($p=0.033$, students t-test, n=6). Levels of total NR1 were not increased with PregS treatment (total NR1 for PregS-treated as a percent of control: 89 ± 10%, $p=0.291$, students t-test, n=6). Na/K ATPase

Molecular Pharmacology Fast Forward. Published on May 28, 2013 as DOI: 10.1124/mol.113.085696
This article has not been copyedited and formatted. The final version may differ from this version.

(Kaplan, 2002; Zhang et al., 2009) and valosin containing protein (VCP) (Zhang et al., 1994; Kobayashi et al., 2002) were used as surface and intracellular markers, respectively. Biotinylated Na/K ATPase was observed in all experiments (n = 6), while biotinylated VCP was below the limit of detection.

Molecular Pharmacology Fast Forward. Published on May 28, 2013 as DOI: 10.1124/mol.113.085696
This article has not been copyedited and formatted. The final version may differ from this version.

Discussion

The ability of nerve cells to regulate receptor number, composition, and distribution is central to nervous system function. Neuronal activity regulates NMDA receptor trafficking via both phosphorylation-dependent and phosphorylation-independent pathways (Chen and Roche, 2007; Lau et al., 2009), and insulin potentiates the NMDA response via the insulin receptor-activated tyrosine kinase (Skeberdis et al., 2001b).

The hypothesis of a linkage between ionotropic glutamate receptors and metabotropic G_i-protein coupled pathways via a "noncanonical" signal transduction mechanism that is not triggered by ion current suggests a pathway for crosstalk between the large classes of ionotropic and metabotropic systems. Results consistent with this can be found in several reports (Rodríguez-Moreno and Sihra, 2007). For example, the treatment of rat cortical neurons in culture with AMPA in the absence of extracellular permeant cations decreases PTx-mediated ADP glycosylation of $G\alpha_{i1}$ and induces rapid association of $G\alpha_{i1}$ with GluR1 AMPA receptors (Wang et al., 1997). Similarly, exposure of mouse dorsal root ganglion neurons to kainate elevates $[Ca^{2+}]_i$ via a PTx-sensitive, phospholipase C-dependent mechanism that is not dependent upon ion permeation, and this effect is absent in neurons from GlurR5-deficient mice (Rozas et al., 2003). A direct interaction with a G-protein seems unlikely as NMDARs do not exhibit homology to GPCR G-protein interacting domains and are not known to interact directly with G-proteins. Direct protein-protein coupling and functional crosstalk between NR1/2A NMDARs and D1 dopamine receptors (Nai et al., 2010; Martina and Bergeron, 2008; Pei et al., 2004) is suggestive of a receptor subtype selective mechanism for crosstalk. This raises the possibility of cell signaling mediated crosstalk.

Molecular Pharmacology Fast Forward. Published on May 28, 2013 as DOI: 10.1124/mol.113.085696
This article has not been copyedited and formatted. The final version may differ from this version.

In this report, the results show that PregS stimulates a sustained increase in the NMDA response that develops over several minutes, rather than milliseconds to seconds, and results from the incorporation of additional functional receptors into the surface membrane. The delayed onset PregS-induced augmentation of the NMDA response is subunit-specific and, unlike the rapid phase of potentiation, requires G-protein coupled activation of PKC and PLC and increased $[Ca^{++}]_i$. When combined with the effect of rapid positive allosteric modulation total enhancement of the NMDA response averages 200% but can reach up to 400% in a given neuron.

Delayed potentiation of the electrophysiological response is mediated by the release of Ca^{2+} from intracellular stores. EGTA, heparin, and thapsigargin inhibit delayed potentiation suggesting a role for $Ca^{2+.}$ Consistent with the results of inhibitors, Ca^{2+} imaging using fluo-3 shows that PregS releases Ca^{2+} from intracellular stores in oocytes expressing NR1/2A receptors. In contrast to some other agents that release intracellular Ca^{2+}, such as acetylcholine (Dascal et al., 1985) and lysophosphatidic acid (Jaconi et al., 1997), PregS does not elicit detectable activation of Ca^{2+}-sensitive chloride current in oocytes, suggesting that PregS induced Ca^{2+} release is localized or limited in magnitude. Oocytes expressing NR1/2D receptors did not exhibit delayed modulation of the NMDA response or PregS-induced Ca^{2+} release, suggesting that the interaction of PregS with NR1/2D receptors is unable to activate the signaling pathway that releases intracellular Ca^{2+} and leads to increased NMDAR surface expression.

BoNT A blocks delayed potentiation, arguing that PregS stimulates delivery of NMDARs to the cell surface by SNARE mediated exocytosis. The vesicular trafficking inhibitor BFA (Klausner et al., 1992), which inhibits NMDA-induced LTP and rapid membrane insertion of AMPA receptor subunits (Broutman and Baudry, 2001), similarly inhibits delayed potentiation, arguing

Molecular Pharmacology Fast Forward. Published on May 28, 2013 as DOI: 10.1124/mol.113.085696
This article has not been copyedited and formatted. The final version may differ from this version.

that NMDARs are inserted into the membrane from an intracellular pool via a functional secretory pathway. The ability of PregS to increase delivery of NMDARs to the cell surface as confirmed by immunoprecipitation of surface-labeled NMDARs, demonstrates a significant increase in surface NR1 subunits following PregS treatment of cortical neurons in culture.

Delayed potentiation is reversed ~3 - 5 min after washout of PregS, suggesting that the additional surface NMDARs are rapidly re-internalized. The PregS-induced increase in surface NMDARs could be due to either stimulation of NMDAR exocytosis or to inhibition of NMDAR endocytosis (Nong et al., 2004). But BoNT A did not reduce the NMDA response in the absence of PregS (data not shown), arguing that the latter is not the case.

Injection of PTx inhibits delayed potentiation, implicating a PTx-sensitive G_i/G_o protein, and blockade of delayed potentiation by U-73122 implicates G protein mediated PLC activation. Although PLC activation is primarily associated with G_q-coupled GPCRs, there is evidence that G_i can also participate in PLC-dependent mobilization of intracellular Ca^{2+}, likely via the $\beta\gamma$ subunit (Mizuta et al., 2011). How PregS activates G-protein coupled signaling pathways to increase surface NMDARs remains unclear. PregS interacts with σ1 receptors that couple to G_i in mouse brain membranes (Ueda et al., 2001), but delayed potentiation is unaffected by the σ1 antagonists BD 1063 and haloperidol, indicating that delayed potentiation in oocytes is not mediated by σ1 receptors.

Application of PregS for 10 min in the absence of NMDA or glutamate increases the response to a subsequent application of NMDA. As PregS alone does not induce a detectable current, activation of the NMDAR channel is not required for delayed potentiation. For the same reason, the increase in $[Ca^{2+}]_i$ observed when PregS alone is applied to oocytes cannot be due to entry of

Molecular Pharmacology Fast Forward. Published on May 28, 2013 as DOI: 10.1124/mol.113.085696
This article has not been copyedited and formatted. The final version may differ from this version.

Ca^{2+} via the NMDAR channel or voltage-gated Ca^{2+} channels. Moreover, delayed potentiation by PregS persists when extracellular Ca^{2+} is replaced with Ba^{2+}, which does not stimulate PKC-mediated enhancement of the NMDA response (Zheng et al., 1997). These findings indicate that PregS induces increased $[Ca^{2+}]_i$ and delayed potentiation of the NMDA response via a pathway that is not dependent upon ion permeation through the NMDAR channel.

Taken together, the results support the model diagrammed in Fig. 10, in which PregS, acting through the NMDAR, stimulates $G_{i/o}$ dependent activation of PLC, resulting in production of diacylglycerol (DAG) and IP_3, thereby triggering Ca^{2+} release from intracellular stores and stimulating Ca^{2+} dependent insertion of NMDARs into the surface membrane. This is similar to the pathway described for potentiation of NMDA responses and NMDAR surface expression by the mGluR agonist (1*S*,3*R*)-1-amino-cyclopentane-1,3-dicarboxylic acid (ACPD) in oocytes co-expressing NR1-4b/NR2A receptors and mGluR1α glutamate receptors (Skeberdis et al., 2001a), which has been reported to mediate postsynaptic long-term potentiation at hippocampal mossy fiber synapses (Kwon and Castillo, 2008). As with delayed potentiation by PregS, enhancement of NMDAR surface expression by ACPD is antagonized by staurosporine, BoToxA, U-73122, or intracellular Ca^{2+} chelation. However, potentiation by ACPD requires co-expression of GluR1α (Lan et al., 2001b; Skeberdis et al., 2001a), whereas delayed potentiation and release of intracellular Ca^{2+} by PregS requires only expression of NR1/2A receptors.

The location of the recognition site responsible for delayed potentiation by PregS remains to be identified. The recognition site for delayed potentiation is likely distinct from the site responsible for rapid potentiation, based on (1) substantially higher affinity of PregS at inducing delayed than rapid potentiation of NR1/2A receptors, (2) delayed potentiation of NR1/2A receptors by

Molecular Pharmacology Fast Forward. Published on May 28, 2013 as DOI: 10.1124/mol.113.085696
This article has not been copyedited and formatted. The final version may differ from this version.

100 nM PregS in the absence of rapid potentiation, and (3) delayed potentiation of NR1-1a/χ4 receptors without rapid potentiation. Another possibility is that the PregS recognition site that mediates delayed potentiation and $[Ca^{2+}]_i$ increase is physically located on another protein, with the NMDAR playing a subunit-specific yet permissive role to enable this interaction.

Movement of receptors from the subsynaptic receptor pool to the synaptic population and the constitutive trafficking of receptors is essential to the viability and functionality of neurons (Lau and Zukin, 2007). Membrane fusion events contribute to NMDA receptor-dependent LTP, which in adult rat brain slices is associated with rapid Src- and PKC-dependent membrane insertion of NMDARs, pointing to a potential role for NMDAR trafficking in synaptic plasticity (Grosshans et al., 2002).

Neuroactive steroids exert modulatory effects on neurotransmission in a variety of systems. PregS is endogenously present in human brain, but its concentration in the extracellular space is unknown (Liere et al., 2004; Gibbs et al., 2006). While most neurosteroids are neutral hydrophobic molecules, PregS is a negatively charged sulfate ester, potentially capable of being stored and selectively released. A PregS-like factor may act as a retrograde messenger to mediate long-term enhancement of AMPA receptor function in neonatal rat hippocampal slices via presynaptic NMDARs (Mameli and Valenzuela, 2006). PregS acts as a cognitive enhancer *in vivo* (Gibbs et al., 2006; Schumacher et al., 2008) and acts both presynaptically and postsynaptically to enhance synaptic transmission in multiple neurotransmitter systems (Zheng, 2009), but the mechanism of these diverse effects is not well understood.

Regulation of intracellular Ca^{2+} release or sequestration is potentially a unifying mechanism to account for the diverse effects of this neuroactive steroid on synaptic transmission, many of

Molecular Pharmacology Fast Forward. Published on May 28, 2013 as DOI: 10.1124/mol.113.085696
This article has not been copyedited and formatted. The final version may differ from this version.

which can be understood in terms of alterations in Ca^{2+}-dependent processes, such as the vesicular release of transmitters or delivery of receptors to the cell surface. The results suggest that in addition to the well-established ionotropic mechanism whereby NMDARs directly transport Ca^{2+} ions, NMDARs are also capable of regulating $[Ca^{2+}]_i$ by engaging a noncanonical metabotropic signaling cascade that in turn increases NMDAR surface expression. PregS induced NMDAR upregulation constitutes a novel mechanism whereby a sulfated neurosteroid or related molecule could act synergistically with direct allosteric modulation of receptor function to profoundly influence synaptic transmission. Such a feed-forward mechanism could provide a positive regulatory mechanism for the augmentation of synaptic activity independent of NMDAR channel activity, with downstream consequences for NMDAR dependent synaptic plasticity and memory.

Regulated trafficking of NMDARs between membrane and intracellular pools is critical for maintenance and plasticity of synaptic connections, and dysregulation of NMDAR trafficking has been implicated in neuropsychiatric disorders (Lau and Zukin, 2007). The present results suggest that NMDAR surface expression is subject to a novel mode of regulation mediated by neuroactive steroids via the NMDA receptor itself, which may play a role in disorders of NMDAR trafficking or provide a basis for development of therapeutic interventions.

Acknowledgements

This work is based on unpublished work by Dr. Mijeong Park-Chung, who first observed delayed potentiation by PregS in neurons; Dr. Nader Yaghoubi, who first replicated delayed potentiation in the *Xenopus* oocyte system; and Dr. Andrew Malayev, who obtained initial evidence indicating a role for PKC.

Molecular Pharmacology Fast Forward. Published on May 28, 2013 as DOI: 10.1124/mol.113.085696
This article has not been copyedited and formatted. The final version may differ from this version.

Authorship Contributions

Participated in research design: Kostakis, Smith, Jang, Martin, Russek, Gibbs, Farb

Conducted experiments: Kostakis, Smith, Jang, Martin, Richards

Contributed new reagents or analytical tools: none

Performed data analysis: Kostakis, Smith, Jang, Richards, Russek, Martin, Gibbs, Farb

Wrote or contributed to the writing of the manuscript: Kostakis, Smith, Russek, Gibbs, Farb

References

Benveniste M and Mayer ML (1995) Trapping of glutamate and glycine during open channel block of rat hippocampal neuron NMDA receptors by 9-aminoacridine. *J Physiol* **483**:367-384.

Berezhnoy D, Gravielle MC, Downing S, Kostakis E, Basile AS, Skolnick P, Gibbs TT and Farb DH (2008) Pharmacological Properties of DOV 315,090, an ocinaplon metabolite. *BMC Pharmacol* **8**:11.

Broutman G and Baudry M (2001) Involvement of the secretory pathway for AMPA receptors in NMDA-induced potentiation in hippocampus. *Journal of Neuroscience* **21**:27-34.

Chen BS and Roche KW (2007) Regulation of NMDA receptors by phosphorylation. *Neuropharmacology* **53**:362-368.

Chen L, Miyamoto Y, Furuya K, Mori N and Sokabe M (2007) PREGS induces LTP in the hippocampal dentate gyrus of adult rats via the tyrosine phosphorylation of NR2B coupled to ERK/CREB [corrected] signaling. *J Neurophysiol* **98**:1538-1548.

Chen N, Luo T and Raymond LA (1999) Subtype-dependence of NMDA receptor channel open probability. *Journal of Neuroscience* **19**:6844-6854.

Dascal N, Gillo B and Lass Y (1985) Role of calcium mobilization in mediation of acetylcholine-evoked chloride currents in *Xenopus laevis* oocytes. *J Physiol* **366**:299-313.

Farb DH, Berg DK and Fischbach GD (1979) Uptake and release of [^{3}H]γ-aminobutyric acid by embryonic spinal cord neurons in dissociated cell culture. *J Cell Biol* **80**:651-661.

Gaspar PA, Bustamante ML, Silva H and Aboitiz F (2009) Molecular mechanisms underlying glutamatergic dysfunction in schizophrenia: therapeutic implications. *J Neurochem* **111**:891-900.

Gibbs TT, Russek SJ and Farb DH (2006) Sulfated steroids as endogenous neuromodulators. *Pharmacol Biochem Behav* **84**:555-567.

Grosshans DR, Clayton DA, Coultrap SJ and Browning MD (2002) LTP leads to rapid surface expression of NMDA but not AMPA receptors in adult rat CA1. *Nature Neuroscience* **5**:27-33.

Horak M, Vlcek K, Chodounska H and Vyklický L (2006) Subtype-dependence of N-methyl-d-aspartate receptor modulation by pregnenolone sulfate. *Neuroscience* **137**:93-102.

Jaconi M, Pyle J, Bortolon R, Ou J and Clapham D (1997) Calcium release and influx colocalize to the endoplasmic reticulum. *Curr Biol* **7**:599-602.

Jang MK, Mierke DF, Russek SJ and Farb DH (2004) A steroid modulatory domain on NR2B controls N-methyl-D-aspartate receptor proton sensitivity. *Proc Natl Acad Sci U S A* **101**:8198-8203.

Kaplan JH (2002) Biochemistry of Na,K-ATPase. *Annu Rev Biochem* **71**:511-535.

Klausner RD, Donaldson JG and Lippincott-Schwartz J (1992) Brefeldin A: insights into the control of membrane traffic and organelle structure. *J Cell Biol* **116**:1071-1080.

Kobayashi T, Tanaka K, Inoue K and Kakizuka A (2002) Functional ATPase activity of p97/valosin-containing protein (VCP) is required for the quality control of endoplasmic reticulum in neuronally differentiated mammalian PC12 cells. *J Biol Chem* **277**:47358-47365.

Kostakis E, Jang MK, Russek SJ, Gibbs TT and Farb DH (2011) A steroid modulatory domain in NR2A collaborates with NR1 exon-5 to control NMDAR modulation by pregnenolone sulfate and protons. *J Neurochem* **119**:486-496.

Kwon HB and Castillo PE (2008) Long-term potentiation selectively expressed by NMDA receptors at hippocampal mossy fiber synapses. *Neuron* **57**:108-120.

Labrie V and Roder JC (2009) The involvement of the NMDA receptor d-serine/glycine site in the pathophysiology and treatment of schizophrenia. *Neurosci Biobehav Rev* **34**:351-372.

Lan JY, Skeberdis VA, Jover T, Grooms SY, Lin Y, Araneda RC, Zheng X, Bennett MV and Zukin RS (2001a) Protein kinase C modulates NMDA receptor trafficking and gating. *Nature Neuroscience* **4**:382-390.

Lan JY, Skeberdis VA, Jover T, Zheng X, Bennett MV and Zukin RS (2001b) Activation of metabotropic glutamate receptor 1 accelerates NMDA receptor trafficking. *Journal of Neuroscience* **21**:6058-6068.

Lau CG, Takeuchi K, Rodenas-Ruano A, Takayasu Y, Murphy J, Bennett MV and Zukin RS (2009) Regulation of NMDA receptor Ca^{2+} signalling and synaptic plasticity. *Biochem Soc Trans* **37**:1369-1374.

Lau CG and Zukin RS (2007) NMDA receptor trafficking in synaptic plasticity and neuropsychiatric disorders. *Nat Rev Neurosci* **8**:413-426.

Liere P, Pianos A, Eychenne B, Cambourg A, Liu S, Griffiths W, Schumacher M, Sjövall J and Baulieu EE (2004) Novel lipoidal derivatives of pregnenolone and dehydroepiandrosterone and absence of their sulfated counterparts in rodent brain. *J Lipid Res* **45**:2287-2302.

Litchfield DW (2003) Protein kinase CK2: structure, regulation and role in cellular decisions of life and death. *Biochem J* **369**:1-15.

Majewska MD and Schwartz RD (1987) Pregnenolone-sulfate: an endogenous antagonist of the gamma-aminobutyric acid receptor complex in brain? *Brain Res* **404**:355-360.

Malayev A, Gibbs TT and Farb DH (2002) Inhibition of the NMDA response by pregnenolone sulphate reveals subtype selective modulation of NMDA receptors by sulphated steroids. *Br J Pharmacol* **135**:901-909.

Mameli M and Valenzuela CF (2006) Alcohol increases efficacy of immature synapses in a neurosteroid-dependent manner. *Eur J Neurosci* **23**:835-839.

Martina M and Bergeron R (2008) D1 and D4 dopaminergic receptor interplay mediates coincident G protein-independent zand dependent regulation of glutamate NMDA receptors in the lateral amygdala. *J Neurochem* **106**:2421-2435.

Martin SC, Russek SJ and Farb DH (1999) Molecular identification of the human GABABR2: cell surface expression and coupling to adenylyl cyclase in the absence of GABABR1. *Mol Cell Neurosci* **13**:180-191.

Marx CE, Bradford DW, Hamer RM, Naylor JC, Allen TB, Lieberman JA, Strauss JL and Kilts JD (2011) Pregnenolone as a novel therapeutic candidate in schizophrenia: emerging preclinical and clinical evidence. *Neuroscience* **191**:78-90.

Marx CE, Keefe RS, Buchanan RW, Hamer RM, Kilts JD, Bradford DW, Strauss JL, Naylor JC, Payne VM, Lieberman JA, Savitz AJ, Leimone LA, Dunn L, Porcu P, Morrow AL and Shampine LJ (2009) Proof-of-concept trial with the neurosteroid pregnenolone targeting cognitive and negative symptoms in schizophrenia. *Neuropsychopharmacology* **34**:1885-1903.

McLean PJ, Shpektor D, Bandyopadhyay S, Russek SJ and Farb DH (2000) A minimal promoter for the GABA(A) receptor alpha6-subunit gene controls tissue specificity. *J Neurochem* **74**:1858-1869.

Milev P, Ho BC, Arndt S and Andreasen NC (2005) Predictive values of neurocognition and negative symptoms on functional outcome in schizophrenia: a longitudinal first-episode study with 7-year follow-up. *Am J Psychiatry* **162**:495-506.

Misumi Y, Miki K, Takatsuki A, Tamura G and Ikehara Y (1986) Novel blockade by brefeldin A of intracellular transport of secretory proteins in cultured rat hepatocytes. *J Biol Chem* **261**:11398-11403.

Mizuta K, Mizuta F, Xu D, Masaki E, Panettieri RA and Emala CW (2011) Gi-coupled γ-aminobutyric acid-B receptors cross-regulate phospholipase C and calcium in airway smooth muscle. *Am J Respir Cell Mol Biol* **45**:1232-1238.

Nai Q, Li S, Wang SH, Liu J, Lee FJ, Frankland PW and Liu F (2010) Uncoupling the D1-N-methyl-D-aspartate (NMDA) receptor complex promotes NMDA-dependent long-term potentiation and working memory. *Biol Psychiatry* **67**:246-254.

Nishizaki T, Matsuoka T, Nomura T, Kondoh T, Tamaki N and Okada Y (1999) Store Ca^{2+} depletion enhances NMDA responses in cultured human astrocytes. *Biochem Biophys Res Commun* **259**:661-664.

Noh SJ, Kim MJ, Shim S and Han JK (1998) Different signaling pathway between sphingosine-1-phosphate and lysophosphatidic acid in Xenopus oocytes: functional coupling of the sphingosine-1-phosphate receptor to PLC-xbeta in Xenopus oocytes. *Journal of Cellular Physiology* **176**:412-423.

Nong Y, Huang YQ and Salter MW (2004) NMDA receptors are movin' in. *Curr Opin Neurobiol* **14**:353-361.

Oda K, Hirose S, Takami N, Misumi Y, Takatsuki A and Ikehara Y (1987) Brefeldin A arrests the intracellular transport of a precursor of complement C3 before its conversion site in rat hepatocytes. *FEBS Lett* **214**:135-138.

Park-Chung M, Wu FS, Purdy RH, Malayev AA, Gibbs TT and Farb DH (1997) Distinct sites for inverse modulation of N-methyl-D-aspartate receptors by sulfated steroids. *Mol Pharmacol* **52**:1113-1123.

Pei L, Lee FJ, Moszczynska A, Vukusic B and Liu F (2004) Regulation of dopamine D1 receptor function by physical interaction with the NMDA receptors. *J Neurosci* **24**:1149-1158.

Pellizzari R, Rossetto O, Schiavo G and Montecucco C (1999) Tetanus and botulinum neurotoxins: mechanism of action and therapeutic uses. *Philos Trans R Soc Lond B Biol Sci* **354**:259-268.

Rodríguez-Moreno A and Sihra TS (2007) Metabotropic actions of kainate receptors in the CNS. *J Neurochem* **103**:2121-2135.

Rozas JL, Paternain AV and Lerma J (2003) Noncanonical signaling by ionotropic kainate receptors. *Neuron* **39**:543-553.

Sabeti J, Nelson TE, Purdy RH and Gruol DL (2007) Steroid pregnenolone sulfate enhances NMDA-receptor-independent long-term potentiation at hippocampal CA1 synapses: Role for L-type calcium channels and sigma-receptors. *Hippocampus* **17**:349-369.

Sadri-Vakili G, Janis GC, Pierce RC, Gibbs TT and Farb DH (2008) Nanomolar concentrations of pregnenolone sulfate enhance striatal dopamine overflow in vivo. *J Pharmacol Exp Ther* **327**:840-845.

Schumacher M, Liere P, Akwa Y, Rajkowski K, Griffiths W, Bodin K, Sjövall J and Baulieu EE (2008) Pregnenolone sulfate in the brain: a controversial neurosteroid. *Neurochem Int* **52**:522-540.

Skeberdis VA, Lan J, Opitz T, Zheng X, Bennett MV and Zukin RS (2001a) mGluR1-mediated potentiation of NMDA receptors involves a rise in intracellular calcium and activation of protein kinase C. *Neuropharmacology* **40**:856-865.

Skeberdis VA, Lan J, Zheng X, Zukin RS and Bennett MV (2001b) Insulin promotes rapid delivery of N-methyl-D- aspartate receptors to the cell surface by exocytosis. *Proc Natl Acad Sci U S A* **98**:3561-3566.

Sliwinski A, Monnet FP, Schumacher M and Morin-Surun MP (2004) Pregnenolone sulfate enhances long-term potentiation in CA1 in rat hippocampus slices through the modulation of N-methyl-D-aspartate receptors. *J Neurosci Res* **78**:691-701.

Smallridge RC, Kiang JG, Gist ID, Fein HG and Galloway RJ (1992) U-73122, an aminosteroid phospholipase C antagonist, noncompetitively inhibits thyrotropin-releasing hormone effects in GH3 rat pituitary cells. *Endocrinology* **131**:1883-1888.

Smith RJ, Sam LM, Justen JM, Bundy GL, Bala GA and Bleasdale JE (1990) Receptor-coupled signal transduction in human polymorphonuclear neutrophils: effects of a novel inhibitor of phospholipase C-dependent processes on cell responsiveness. *Journal of Pharmacology and Experimental Therapeutics* **253**:688-697.

Thompson AK, Mostafapour SP, Denlinger LC, Bleasdale JE and Fisher SK (1991) The aminosteroid U-73122 inhibits muscarinic receptor sequestration and phosphoinositide hydrolysis in SK-N-SH neuroblastoma cells. A role for Gp in receptor compartmentation. *J Biol Chem* **266**:23856-23862.

Ueda H, Yoshida A, Tokuyama S, Mizuno K, Maruo J, Matsuno K and Mita S (2001) Neurosteroids stimulate G protein-coupled sigma receptors in mouse brain synaptic membrane. *Neurosci Res* **41**:33-40.

Wang Y, Small DL, Stanimirovic DB, Morley P and Durkin JP (1997) AMPA receptor-mediated regulation of a Gi-protein in cortical neurons. *Nature* **389**:502-504.

Whittaker MT, Gibbs TT and Farb DH (2008) Pregnenolone sulfate induces NMDA receptor dependent release of dopamine from synaptic terminals in the striatum. *J Neurochem* **107**:510-521.

Wu FS, Gibbs TT and Farb DH (1991) Pregnenolone sulfate: a positive allosteric modulator at the N-methyl-D-aspartate receptor. *Mol Pharmacol* **40**:333-336.

Yao Y, Choi J and Parker I (1995) Quantal puffs of intracellular Ca2+ evoked by inositol trisphosphate in Xenopus oocytes. *J Physiol* **48 (Pt 3)**:533-553.

Zhang D, Hou Q, Wang M, Lin A, Jarzylo L, Navis A, Raissi A, Liu F and Man HY (2009) Na,K-ATPase activity regulates AMPA receptor turnover through proteasome-mediated proteolysis. *J Neurosci* **29**:4498-4511.

Zhang L, Ashendel CL, Becker GW and Morré DJ (1994) Isolation and characterization of the principal ATPase associated with transitional endoplasmic reticulum of rat liver. *J Cell Biol* **127**:1871-1883.

Zheng P (2009) Neuroactive steroid regulation of neurotransmitter release in the CNS: action, mechanism and possible significance. *Prog Neurobiol* **89**:134-152.

Zheng X, Zhang L, Wang AP, Bennett MV and Zukin RS (1997) Ca2+ influx amplifies protein kinase C potentiation of recombinant NMDA receptors. *J Neurosci* **17**:8676-8686.

Molecular Pharmacology Fast Forward. Published on May 28, 2013 as DOI: 10.1124/mol.113.085696
This article has not been copyedited and formatted. The final version may differ from this version.

Footnotes

Emmanuel Kostakis and Conor Smith contributed equally and are co-first authors.

Terrell T. Gibbs and David H. Farb contributed equally.

Support was provided by National Institute of Mental Health [R01MH049469] and National Institute of General Medical Sciences [T32GM008541] to DHF.

Reprint requests: David H. Farb, Ph.D., Dept. of Pharmacology & Experimental Therapeutics, Boston University School of Medicine, 72 East Concord St., Boston MA 02118, dfarb@bu.edu

Molecular Pharmacology Fast Forward. Published on May 28, 2013 as DOI: 10.1124/mol.113.085696
This article has not been copyedited and formatted. The final version may differ from this version.

Legends for Figures

Fig. 1. PregS induces delayed onset potentiation of the NMDA response in neurons. PregS (100 μM) and NMDA are applied by pressure ejection to primary embryonic spinal cord neurons in culture while recording by whole-cell voltage clamp. (A) Potentiation of the NMDA response by PregS increases upon continued exposure to PregS and typically levels off after about 85 s. Typical results are shown. Two minutes elapsed between the initial control application of NMDA and the beginning of PregS application; 4.5 min elapsed between the termination of PregS application and the final control NMDA response. (B) Delayed enhancement of the NMDA induced current by PregS persists when Ba^{2+} is substituted for Ca^{2+}in the perfusion buffer. (C) Delayed increase in the NMDA induced current by PregS persists when PregS is included in the intracellular electrode buffer. A minimum of 1 min was allowed after establishment of the high resistance seal on the chick spinal cord neurons to permit equilibration of PregS.

Fig. 2. Delayed onset potentiation by PregS is recapitulated by recombinant NMDARs expressed in oocytes. PregS and NMDA are applied by bath perfusion to oocytes expressing NR1/2A subunits while recording in the two-electrode whole-cell voltage clamp mode. (A) Potentiation of the NMDA response by PregS increases upon continued exposure to PregS and typically levels off after 7 – 10 min. Black bars indicate successive applications of NMDA (300 μM). Breaks between traces are 1.3 - 1.8 min (see panel B for times). PregS (100 μM) was added to the perfusion buffer at t = 0 and included for 7 min (overlying black bar). (B) Peak NMDA induced currents determined as in (A) are normalized to the average response before application of PregS beginning at t = 0. Smooth curve reflects an exponential fit (τ = 184 sec). Error bars

Molecular Pharmacology Fast Forward. Published on May 28, 2013 as DOI: 10.1124/mol.113.085696
This article has not been copyedited and formatted. The final version may differ from this version.

indicate S.E.M. (n = 3). Arrows indicate rapid and delayed components of potentiation. Unless otherwise indicated, NMDA (300 μM) and PregS (100 μM) in 0.5% DMSO were used with *Xenopus* oocytes as the standard test concentrations below. Oocytes were perfused with Ba-Ringer and voltage-clamped at –70 mV.

Fig. 3. Delayed potentiation by PregS is independent of fast potentiation and selective for NR1/2A (and NR1/2B). (A) Delayed potentiation is observed with NR1/(2A or 2B) but not NR1/(2C or 2D) or the NR1/NR2D-B chimera (χ4) that is inactive with respect to fast potentiation. NR1 cRNA was co-expressed in oocytes with cRNA for the NR2A, NR2B, NR2C, NR2D or χ4 subunit. Peak currents elicited by application of NMDA + PregS, either simultaneously or after 10 min perfusion with PregS, are expressed relative to the NMDA-induced current in the absence of PregS. * Indicates a significant ($p < 0.001$, paired 2-tail t-test) increase over simultaneous addition of PregS and NMDA. Error bars indicate S.E.M. (n = 7 - 12). (B) Concentration-effect curves for rapid (EC_{50} 21 μM) and delayed (EC_{50} 850 nM) increase in NR1/2A receptors. To measure rapid potentiation, oocytes were exposed simultaneously to 300 μM NMDA plus the indicated concentration of PregS. To measure delayed potentiation, oocytes were perfused for 10 min with the indicated concentration of PregS, then exposed to NMDA + PregS. Delayed potentiation is defined as the additional percentage potentiation of the peak NMDA response after 10 min relative to the response when PregS and NMDA are applied simultaneously. Arrows indicate EC_{50}. Error bars indicate S.E.M. (n = 5 - 7) (C) Concentration-effect curves for rapid (EC_{50} 19 μM) and delayed (EC_{50} 33 μM) potentiation with NR1/2B receptors indicate lower potency but higher efficacy for delayed potentiation by PregS. Arrows indicate EC_{50}. Error bars indicate S.E.M. (n = 5 – 7 oocytes).

Molecular Pharmacology Fast Forward. Published on May 28, 2013 as DOI: 10.1124/mol.113.085696
This article has not been copyedited and formatted. The final version may differ from this version.

Fig. 4. Delayed potentiation but not rapid potentiation is induced by 100 nM PregS in oocytes expressing NR1/2A receptors. Using a reduced concentration of 100 nM PregS, substantial delayed potentiation is observed without detectable rapid potentiation. (A) Typical responses of oocytes expressing NR1/2A receptors to 10 μM NMDA alone, 10 μM NMDA + 100 nM PregS (applied simultaneously), and 10 μM NMDA + 100 nM PregS after 10 min preincubation with 100 nM PregS. (B) Averaged values of normalized peak current responses for rapid and delayed increase in NR1/2A receptors (n = 8 - 10). When added simultaneously with NMDA, PregS produced negligible potentiation of the NMDA response (1 ± 2%), whereas after 10 min preincubation with 100 nM PregS the response to NMDA was enhanced by 45 ± 3% Error bars represent S.E.M (n = 8 - 10). * Indicates a significant difference between rapid and delayed potentiation, $p<0.0005$.

Fig. 5. PregS induces intracellular Ca^{2+} increases in oocytes expressing NR1/2A but not NR1/2D receptors. Cells were injected with 50 nl 1 mM fluo-3 Ca^{2+} indicator and changes in fluorescence during an exposure to PregS were monitored by confocal microscopy. Cells expressing NR1/2A (A - D) exhibit a visible increase in fluorescence near the membrane after PregS application. However, oocytes expressing NR1/2D (E - H) and control oocytes (injected with water vehicle without cRNA) (I - L) do not respond to PregS. Images of NR1/2A (A-C), NR1/2D (E - G) and control oocytes (I - K) before PregS (A, E, I) and after PregS application (B, C, F, G, J and K). The average response to PregS for NR1/2A (D), NR1/2D (H) and control oocytes (L) is represented to the right of the *Xenopus* oocytes images (n = 8).

Fig. 6. PregS induces Ca^{2+} release in neocortical neurons. Neocortical cells isolated from E18 rat maintained in vitro for one week were incubated with fluo-4 Ca^{2+} indicator. Change in

Molecular Pharmacology Fast Forward. Published on May 28, 2013 as DOI: 10.1124/mol.113.085696
This article has not been copyedited and formatted. The final version may differ from this version.

fluorescence (ΔF, arbitrary units) during an exposure to PregS (50 μM in 0.05% DMSO) was monitored by confocal microscopy. Images of neocortical cells in phase (A), phase with Fluo-4 (B) and with Fluo-4 (C). Neocortical Cells exhibit a visible increase in fluorescence in the cell body and processes after PregS treatment (D, E, H and I). Cells exhibit no significant change in fluorescence after vehicle treatment (K and L). Images of cells before (D and H) and after (E and I) PregS treatment, and before (K) and after (L) vehicle treatment are shown. The time course of the responses to PregS of selected cell bodies, designated by arrows in panel D, and of the entire field are shown in panels F and G, respectively. The time course of the response to PregS of a neocortical cell process, designated by the arrowhead in panel H, is shown in panel J. The time course of the response to vehicle application of selected cell bodies (designated by arrows in panel K) and of the entire field are shown in panels M and N, respectively. Scale bar, 10 μm.

Fig. 7. Delayed potentiation of the NMDA response by PregS requires exocytosis of NMDARs. (A) Prior exposure to PregS for 10 min enhances whole-cell currents elicited by co-application of NMDA and PregS to oocytes expressing NR1/2A receptors. V_h = -70 mV. (B) Microinjection of BoNT A (50 ng, 5 h before recording) reduces PregS induced delayed potentiation without affecting rapid potentiation. BoNT A was reduced with 20 mM DTT at room temperature 1 h before use. Controls were injected with 10 mM DTT in 1 mg/ml BSA (n = 10). (C) BoNT A reduces delayed potentiation ($p < 0.00001$, n = 9) with no effect on rapid potentiation. Error bars represent s.e.m based upon the number of oocytes tested.

Fig. 8. PregS increases the number of functional surface NMDARs in oocytes expressing NR1/2A receptors. (A) NMDA (300 μM) and 9-AA (100 μM) co-applied to oocytes expressing

Molecular Pharmacology Fast Forward. Published on May 28, 2013 as DOI: 10.1124/mol.113.085696
This article has not been copyedited and formatted. The final version may differ from this version.

NR1/2A receptors result in a transient inward current as NMDA activated channels are blocked by 9-AA (a voltage dependent open channel blocker). As the holding potential is switched from –70 to +70 mV, an outward tail current reflecting 9-AA unblock of NMDAR channels ensues (black traces). Cells were then exposed to (B) vehicle (Ba-Ringer) or (C) PregS for 10 min and the 9-AA block and unblock sequences repeated (blue traces). Peak tail currents after baseline subtraction are expressed relative to the control current (black trace) from the same cell (p2/p1). (D) The peak current ratio p2/p1 for PregS treated oocytes (blue bar, n = 8) is significantly higher than for vehicle treated oocytes (white bar, n = 6). * Relative current $p < 0.00001$, unpaired 2-tail t-test.

Fig. 9. PregS increases surface NR1 subunits on neocortical neurons. (A) Representative immunoblot of surface NR1 levels in neocortical neurons exposed to PregS for 10 min as compared with vehicle. Surface biotinylated proteins were affinity-purified and analyzed with a fraction of total cellular proteins by immunoblotting with antisera to NR1, surface Na^+/K^+ ATPase (positive control), or cytoplasmic VCP (negative control). (B) Quantitation of the effect of PregS (50 μM, 0.1% DMSO, 10 min) on total and surface-biotinylated NR1. (Left panel) Immunoreactivity in biotinylated aliquots as a fraction of total NR1 expressed as percent of vehicle. PregS induced a 62 ± 25% increase ($p = 0.033$, n = 6 experiments, students t-test) in the biotinylated fraction of NR1. (Right panel) There was no change in total NR1 levels with PregS treatment ($p = 0.291$, n = 6 experiments, students t-test).

Fig. 10. Model of signal transduction pathway for delayed onset potentiation of the NMDA response by PregS. Diagram illustrates the proposed intracellular pathways that participate in the PregS stimulated trafficking of functional NMDA receptors to the cell surface via a non-

Molecular Pharmacology Fast Forward. Published on May 28, 2013 as DOI: 10.1124/mol.113.085696
This article has not been copyedited and formatted. The final version may differ from this version.

canonical G-protein, PLC, Ca^{++} and PKC dependent mechanism.

Molecular Pharmacology Fast Forward. Published on May 28, 2013 as DOI: 10.1124/mol.113.085696
This article has not been copyedited and formatted. The final version may differ from this version.

Tables

Table 1. Second messenger pathways

Treatment	Target	Total Potentiation $\left(\frac{I_{NMDA+PS(10\,\mathrm{min})}}{I_{NMDA}}-1\right)\times 100$	Rapid Potentiation $\left(\frac{I_{NMDA+PS(simul.)}}{I_{NMDA}}-1\right)\times 100$	Delayed Potentiation $\left(\frac{I_{NMDA+PS(10\,\mathrm{min})}}{I_{NMDA+PS(simul.)}}-1\right)\times 100$
Vehicle		203 ± 15%	68 ± 4%	76 ± 7% (15)
PTx	G_i/G_o	140 ± 13%	72 ± 4%	40 ± 6% (13) †
U-73343	inactive control	182 ± 17%	62 ± 6%	75 ± 7% (6)
U-73122	PLC	83 ± 6%	60 ± 5%	14 ± 5% (8) **

Table 1. Cells were treated with the indicated inhibitor prior to measuring the increase in peak response to NMDA (300 µM) produced by PregS (100 µM). Treatment conditions were: U-73122/U-73343, 1 h, 20µM in Barth's solution plus 0.4% DMSO; PTx, 50 nl injection of 500 pg PTx in 5 mM Tris, 0.05 mM EDTA, 0.015% CHAPS, pH 8. Statistically significant vs. vehicle (2-tailed t-test): ** $p < 0.005$; † $p < 0.001$.

Molecular Pharmacology Fast Forward. Published on May 28, 2013 as DOI: 10.1124/mol.113.085696
This article has not been copyedited and formatted. The final version may differ from this version.

Table 2. Intracellular signal transduction pathways

Treatment	Target	Total Potentiation	Rapid Potentiation	Delayed Potentiation
Vehicle		189 ± 8%	65 ± 3%	75 ± 2% (7)
PMA	PKC	76 ± 5%	65 ± 3%	6 ± 1% (8) *
Staurosporine	protein kinase	111 ± 7%	67 ± 2%	25 ± 3% (8)
DRB	casein kinase	173 ± 3%	60 ± 5%	71 ± 6% (4)
Genistein	nonreceptor protein kinase	184 ± 6%	64 ± 4%	73 ± 3% (5)
Vehicle		199 ± 8%	66 ± 5%	81 ± 5% (8)
Bisindolyl-maleimide I	PKC	118 ± 12%	65 ± 3%	31 ± 7% (8) **
H89	PKA	204 ± 9%	63 ± 3%	87 ± 4% (6)
Vehicle		226 ± 18%	70 ± 4%	91 ± 6% (8)
U-0126	MEK	232 ± 22%	77 ± 8%	91 ± 6% (6)
Vehicle		194 ± 19%	64 ± 8%	79 ± 8% (6)
Tyrphostin A47	insulin receptor tyr kinase	210 ± 24%	72 ± 8%	80 ± 9% (6)

Table 2. Cells were treated with the indicated pharmacological inhibitor prior to measuring the rapid and delayed (10 min) increase in peak response to NMDA (300 μM) produced by PregS (100 μM). Treatment conditions were: PMA, 10 min, 2 μM in Barth's solution plus 0.5% DMSO; Bisindolylmaleimide I, 2-3 h, 2 μM in Barth's solution plus 0.5% DMSO; H-89, 1-2 h, 4 μM in Barth's solution plus 0.5% DMSO; Staurosporine, 2h, 2 μM in Barth's solution plus 0.5% DMSO; DRB, 2h, 60 μM in Barth's solution plus 0.5% DMSO; genistein, 2h, 50 μM in Barth's solution plus 0.5% DMSO; U-0126, 1 h, 20 μM in Barth's solution plus 1% DMSO; Tyrphostin A47, 20 min, 100 μM in Barth's solution plus 0.5% DMSO. Statistically significant vs. vehicle (2-tailed t-test): * $p < 0.01$; ** $p < 0.005$.

Molecular Pharmacology Fast Forward. Published on May 28, 2013 as DOI: 10.1124/mol.113.085696
This article has not been copyedited and formatted. The final version may differ from this version.

Table 3. Calcium signaling

Treatment	Target	Total Potentiation	Rapid Potentiation	Delayed Potentiation
de-N-sulfated heparin	inactive control	227 ± 26%	77 ± 7%	91 ± 9% (8)
Heparin	IP_3 receptor	110 ± 8%	86 ± 7%	12 ± 5% (9) **
Vehicle		208 ± 19%	61 ± 7%	91 ± 7% (10)
EGTA	$[Ca^{2+}]_i$	111 ± 9%	69 ± 5%	25 ± 5% (11) **
Vehicle		197 ± 15%	72 ± 5%	74 ± 6% (7)
Thapsigargin	SERCA	101 ± 6%	73 ± 5%	16 ± 4% (8) †

Table 3. Cells were treated with the indicated inhibitor prior to measuring the rapid and delayed (10 min) increase in peak response to NMDA (300 μM) produced by PregS (100 μM). Treatment conditions were: EGTA, 50 nl injection of 5 mM EGTA in water; heparin/de-N-sulfated heparin, 1 mM, 50 nl injection; thapsigargin, 1 h, 1 mM in Barth's solution plus 0.1% DMSO.

Statistically significant vs. vehicle (2-tailed t-test): ** $p < 0.005$; † $p < 0.001$.

Figure 1

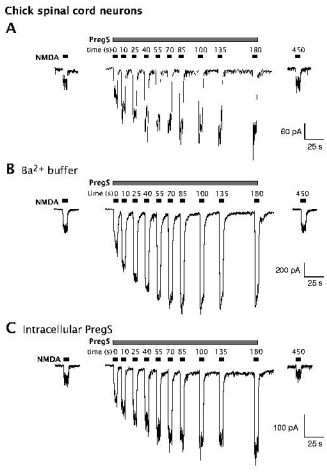
Chick spinal cord neurons
A
PregS
time (s) 0 10 25 40 55 70 85 100 135 180 450
NMDA
60 pA
25 s
B Ba2+ buffer
PregS
time (s) 0 10 25 40 55 70 85 100 135 180 450
NMDA
200 pA
25 s
C Intracellular PregS
PregS
time (s) 0 10 25 40 55 70 85 100 135 180 450
NMDA
100 pA
25 s

Figure 2

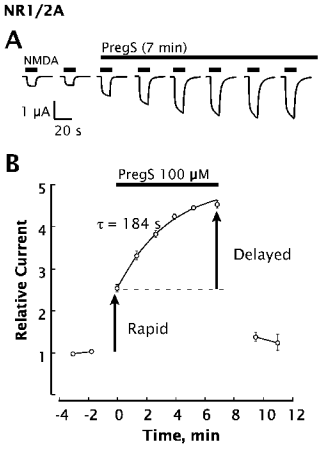
NR1/2A
A
NMDA
PregS (7 min)
1 μA
20 s
B
PregS 100 μM
τ = 184 s
Delayed
Rapid
Relative Current
1
2
3
4
5
-4
-2
0
2
4
6
8
10
12
Time, min

Figure 3

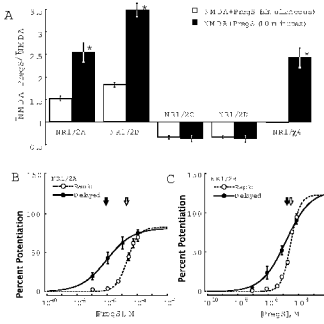

Figure 4

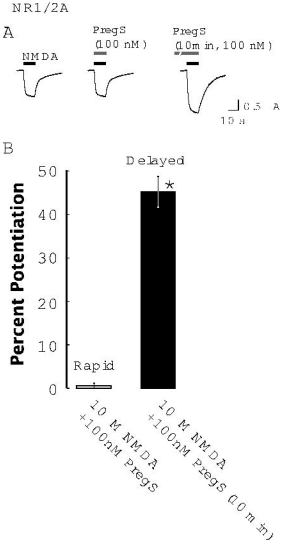
NR1/2A
A
NMDA
PregS
(100 nM)
PregS
(10m in, 100 nM)
0.5 A
10 s
B
Delayed
Percent Potentiation
50
40
30
20
10
0
Rapid
10 M NMDA
+100nM PregS
10 M NMDA
+100nM PregS (10 min)

Figure 5

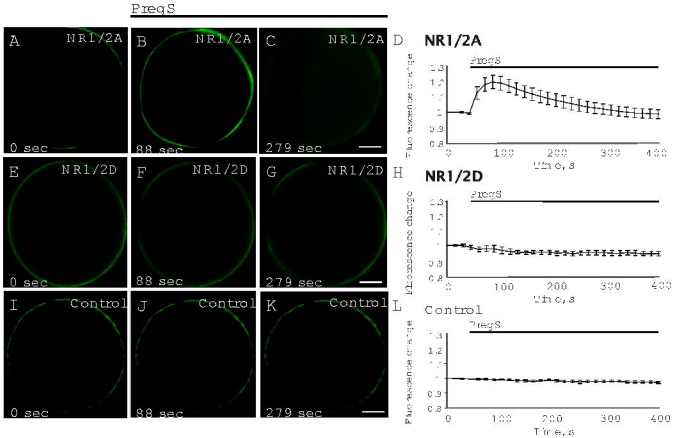
PreqS
A NR1/2A
B NR1/2A
C NR1/2A
D
NR1/2A
0 sec
88 sec
279 sec
PreqS
E NR1/2D
F NR1/2D
G NR1/2D
H
NR1/2D
0 sec
88 sec
279 sec
I Control
J Control
K Control
L
Control
0 sec
88 sec
279 sec
Time, s

Figure 6

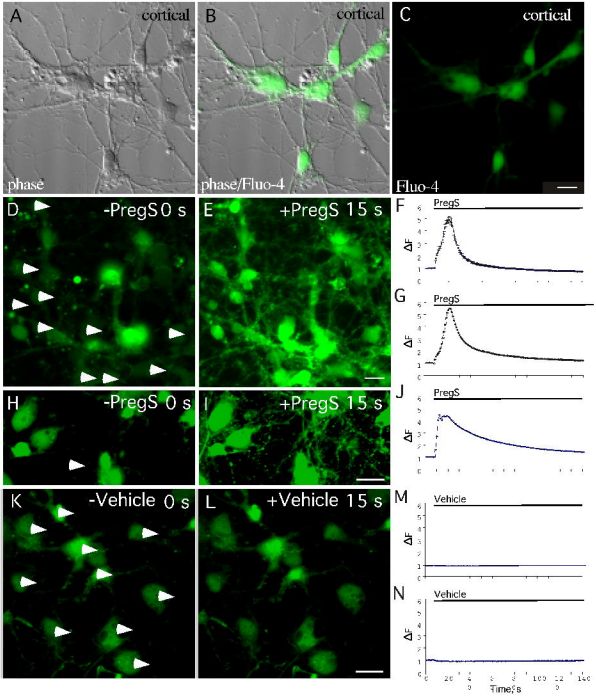
A
cortical
phase
B
cortical
phase/Fluo-4
C
cortical
Fluo-4
D
-PregS 0 s
E
+PregS 15 s
F
PregS
ΔF
G
PregS
ΔF
H
-PregS 0 s
I
+PregS 15 s
J
PregS
ΔF
K
-Vehicle 0 s
L
+Vehicle 15 s
M
Vehicle
ΔF
N
Vehicle
ΔF
Time/s

Figure 7

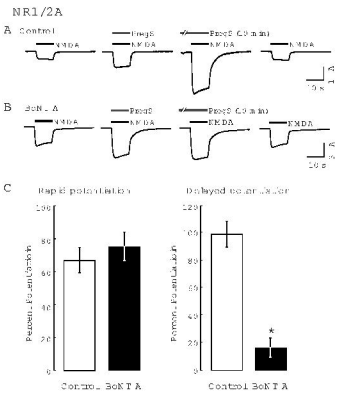
NR1/2A
A Control
NMDA
NMDA
NMDA
NMDA
10 s
B BoNT A
NMDA
NMDA
NMDA
NMDA
10 s
C
Rapid potentiation
Delayed potentiation
Percent Potentiation
Percent Potentiation
Control BoNT A
Control BoNT A
*

Figure 8

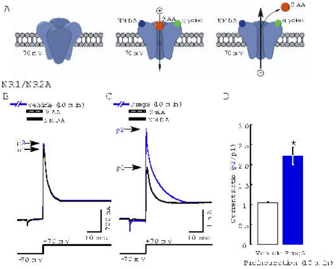
A
NMDA
9 AA
NR1/NR2A
B
C
D
Vehicle (10 min)
PregS (10 min)
p2
p1
10 sec
+70 mV
-70 mV
Vehicle
PregS
Preincubation (10 min)

Figure 9

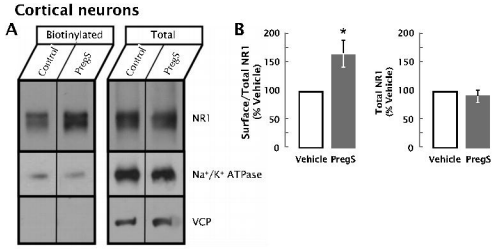
Cortical neurons
A
Biotinylated
Total
Control
PregS
Control
PregS
NR1
Na+/K+ ATPase
VCP
B
Surface/Total NR1 (% Vehicle)
200
150
100
50
0
*
Vehicle
PregS
Total NR1 (% Vehicle)
200
150
100
50
0
Vehicle
PregS

Figure 10

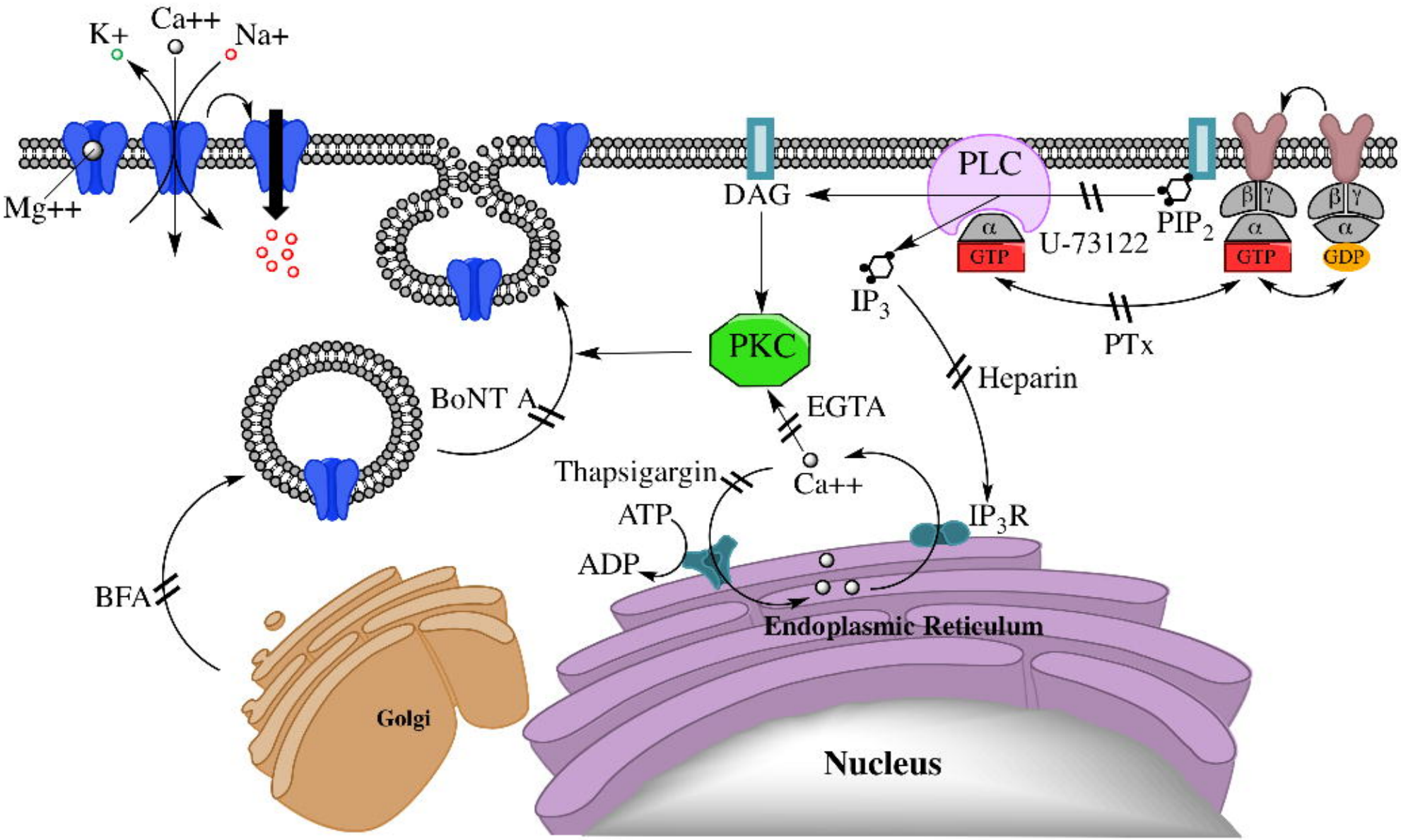
K+
Ca++
Na+
Mg++
PLC
DAG
PIP2
U-73122
α
GTP
β γ
α
GTP
β γ
α
GDP
IP3
PTx
PKC
Heparin
BoNT A
EGTA
Thapsigargin
Ca++
ATP
ADP
IP3R
BFA
Endoplasmic Reticulum
Golgi
Nucleus